of the lactones over the entire pH range investigated.

Registry No. 4 (X = F), 84944-93-4; **5** (X = F), 84944-94-5; **6a**, 41167-81-1; **6d**, 84944-95-6; **6e**, 84944-96-7; **6n**, 84944-97-8; **6o**, 84944-98-9; **7a**, 29423-72-1; **7b**, 84944-99-0; **7c**, 50442-68-7; **7d**, 84945-00-6; **7e**, 84945-01-7; **7f**, 40662-76-8; **7g**, 84959-63-7; **7h**, 84945-02-8; **7i**, 84945-03-9; **7j**, 84945-04-0; **7k**, 40662-32-6; **7l**, 84945-05-1; **7m**, 84945-06-2; **7p**, 84945-07-3; **7q**, 84945-08-4; **7r**, 84945-09-5; **8a**, 84945-10-8; **8g**, 84945-11-9; **9a**, 84945-12-0; **9c**, 84945-13-1; **9f**, 84945-14-2; **9g**, 84945-15-3; **9h**, 84945-16-4; **9k**, 84945-17-5; **9l**, 84945-18-6; **11a**, 84945-19-7; **11c**, 84945-20-0; **11f**, 84959-64-8; **11g**, 84945-21-1; **11h**, 84945-22-2; **11k**, 84945-23-3; **12**, 41167-82-2; **14**, 84945-24-4; **15**, 84945-25-5; **16**, 84945-26-6; 3,5-difluorophenol, 2713-34-0; 1,3,5-trifluorobenzene, 372-38-3; 3,5-difluorophenol α-naphthyl urethane derivative, 84945-27-7; 3,3-dimethylacryloyl chloride, 3350-78-5; 2,6-difluorohydroquinone, 84959-65-9; 2,6-difluorophenol, 28177-48-2; methyl 3,3-dimethylacrylate, 924-50-5; 2,6-diiodohydroquinone, 1955-21-1; 2-methylhydroquinone, 95-71-6; 2,5-dimethylhydroquinone, 615-90-7; 2,3-dimethylhydroquinone, 608-43-5; 2,6-dimethylhydroquinone, 654-42-2; hydroquinone, 123-31-9.

Stereopopulation Control. 8. Rate and Equilibrium Enhancement in the Formation of Homophthalic Anhydrides

Paul S. Hillery and Louis A. Cohen*

Contribution from the Laboratory of Chemistry, National Institute of Arthritis, Diabetes, Digestive and Kidney Diseases, National Institutes of Health, Bethesda, Maryland 20205.
Received July 22, 1982

Abstract: The kinetics of cyclization of α,α,3,4,6-pentamethylhomophthalic acid have been measured in solvent acetonitrile at 28.5 °C, using as catalysts a series of acids ranging in strength from perchloric to acetic. In the presence of 0.12 M $HClO_4$, $t_{1/2}$ for acid anhydride formation = 0.3 s. For the stronger acid catalysts, k_{cycl} is a linear function of catalyst concentration; for the weak acids, however, a change in rate-limiting step is revealed by curvature in the plots of k^{tot}_{obsd} vs. [catalyst]. All the weak acids show the same limiting value, 6.45×10^{-3} min^{-1}; this value is considered to be the rate constant for uncatalyzed formation of the tetrahedral intermediate. Homoconjugate bases (HA_2^-) of the weak acids show a similar curvature in their dilution plots, and the same limiting rate constant as for weak acids. Two independent and competitive pathways for cyclization are proposed. For strong acid catalysis, an intermediate acylium ion is considered on the basis of Brønsted $\alpha = -0.79$, $k_H/k_D \simeq 1$, and acceleration of anhydride hydrolysis by methyl substituents. A value of $\Delta S^{\ddagger} = -23$ eu suggests that cyclization, rather than acylium ion formation, is rate limiting. For weak acid catalysis, $\alpha = -0.17$, $k_H/k_D = 4.3$, $\Delta S^{\ddagger} = -31$ eu, and methyl groups retard anhydride hydrolysis by electron release; for this pathway, catalyzed breakdown of a tetrahedral intermediate is considered rate limiting. The composite Brøsted plot is curved because the two pathways follow different rate laws. In contrast to rate enhancement results for phenolic lactone formation, the pentamethylhomophthalic acid is only sevenfold as reactive as α,α-dimethylhomophthalic acid. For the catalyst acids, pK(acetonitrile) is shown to be a linear function of p$K(H_2O)$ over the entire range of acids examined.

Severe restriction of conformational mobility (stereopopulation control) has been shown to enhance both rate and equilibrium constants for cyclization in intramolecularly reactive systems.[1-4] Quantitative data have already been reported for the formation of benzylic[3a] and phenolic[1,3,4] lactones, phenolic ethers,[5] and lactones resulting from carboxyl addition to double bonds.[6] In our earlier reports, we argued that stereopopulation control serves, primarily, to raise the free energy content of the starting material over that of an analogous system with greater conformational mobility. It should be possible, therefore, to utilize the potential of the energy-rich system to drive the formation of bonds which, in acylic analogues, are recognized as "high-energy."[7] Earlier studies[8] have shown, for example, that both rate and equilibrium constants for the formation of cyclic acid anhydrides (succinic, maleic, phthalic) can be enhanced by the introduction of moderately bulky substituents, suitably placed to limit some degree of rotational freedom.[9] We have now extended these studies to include the formation of homophthalic anhydrides, thiolactones,[10]

Scheme I

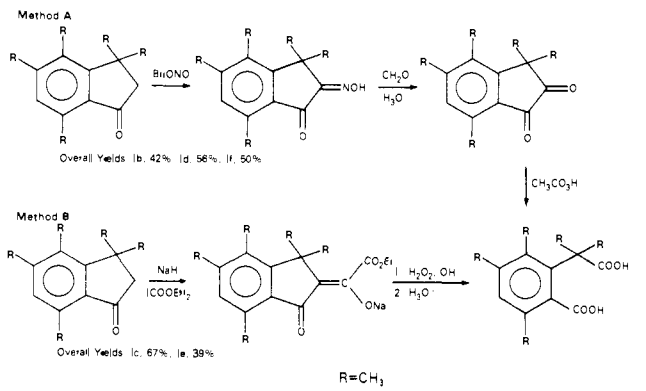

(1) For paper VII, see King, M. M.; Cohen, L. A. *J. Am. Chem. Soc.*, preceding paper in this issue.

(2) For comprehensive discussions of intramolecular facilitation and reviews of earlier data, see (a) Capon, B.; McManus, S. P. "Neighboring Group Participation"; Plenum Press: New York, 1976; Vol. I, Chapter 2. (b) Kirby, A. J. *Adv. Phys. Org. Chem.* **1980**, *17*, 183.

(3) (a) Milstien, S.; Cohen, L. A. *J. Am. Chem. Soc.* **1972**, *94*, 9158. (b) Milstien, S.; Cohen, L. A. *Ibid.* **1970**, *92*, 4377.

(4) Caswell, M.; Schmir, G. L. *J. Am. Chem. Soc.* **1980**, *102*, 4815.

(5) Borchardt, R. T.; Cohen, L. A. *J. Am. Chem. Soc.* **1972**, *94*, 9175.

(6) (a) Borchardt, R. T.; Cohen, L. A. *J. Am. Chem. Soc.* **1972**, *94*, 9175. (b) Borchardt, R. T.; Cohen, L. A. *Ibid.* **1973**, *95*, 8319.

(7) Mahler, H. R.; Cordes, E. H. "Biological Chemistry"; Harper & Row: New York, 1966; p 213 and references cited therein.

(8) Eberson, L.; Welinder, H. *J. Am. Chem. Soc.* **1971**, *93*, 5821.

(9) As we[3] and others[8] have emphasized, conformational restriction is the basis for a number of consequences, all of which may lead to enhancement phenomena.

(10) Blum, M.; Cohen, L. A., manuscript in preparation.

Table I. Equilibria in Homophthalic Anhydride Formation[a]

acid	catalyst	2, %	K_{eq},[b] M	K_{eq} (av)	K_{eq} (rel)
1a	0.20 M CH_3SO_3H (0.032)[c]	10	3.62×10^{-3}	3.62×10^{-3}	1
	0.12 M $HClO_4$ (0.42)	0.85[d]			
1b	0.20 M CH_3SO_3H (0.032)	21	8.84×10^{-3}		
	0.12 M $HClO_4$ (0.42)	2	8.57×10^{-3}	8.71×10^{-3}	2.4
1c	0.20 M CH_3SO_3H (0.032)	69	8.04×10^{-2}		
	0.12 M $HClO_4$ (0.42)	16	8.02×10^{-2}	8.03×10^{-2}	22.2
1d	0.20 M CH_3SO_3H (0.032)	71	8.88×10^{-2}		
	0.12 M $HClO_4$ (0.42)	18	9.24×10^{-2}		
	0.08 M $HClO_4$ (0.28)	24	8.89×10^{-2}		
	0.78 M CF_3COOH (0.13)	41	9.20×10^{-2}	9.05×10^{-2}	25.0
1e	0.012 M CH_3SO_3H (0.016)	98	1.08		
	0.008 M $HClO_4$ (0.028)	97	1.09		
	0.12 M $HClO_4$ (0.42)	72	1.09		
	0.42 M CF_3COOH (0.084)	92	1.09		
	0.73 M CF_3COOH (0.13)	89	1.10		
	0.42 M HCF_2COOH (0.10)	91	1.09	1.09	300
1f	0.12 M $HClO_4$ (0.42)	97	13.58		
	0.18 M $HClO_4$ + 10% H_2O (6.21)	68	13.20		
	0.73 M CF_3COOH (0.13)	99	12.87	13.2	3650

[a] At 28.5 °C in acetonitrile. [b] Calculated as $[2][H_2O]/[1]$. [c] Figures in parentheses give molarity of water present. [d] Calculated from K_{eq} obtained from the preceding set of conditions.

and cyclic acylimidazoles.[11] With respect to both rate and equilibrium, cyclizations of homophthalic acids might be less favorable than those of the previously studied diacids, because of their greater possibilities for rotational isomerism; on the other hand, the six-membered homophthalic anhydrides should be less strained than the analogous phthalic anhydrides and either factor could be the more significant.

Results

Synthesis. Of the six homophthalic acids (**1a–f**) and their anhydrides (**2a–f**) used in this study, only **1a** and **2a** were commerically available. Compounds **1b**, **2b**, **1e**, and **2e** have already

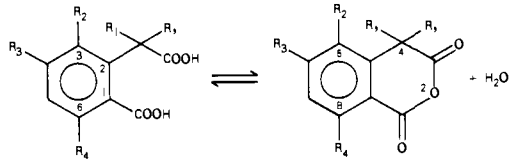

1 2

a, $R_1 = R_2 = R_3 = R_4 = H$ **d**, $R_1 = R_3 = H$; $R_2 = R_4 = CH_3$
b, $R_1 = R_2 = R_3 = H$; $R_4 = CH_3$ **e**, $R_1 = CH_3$; $R_2 = R_3 = R_4 = H$
c, $R_1 = R_3 = R_4 = H$, $R_2 = CH_3$ **f**, $R_1 = R_2 = R_3 = R_4 = CH_3$

been described in early literature; our syntheses of **1b–f**, however, involve combinations of procedures introduced more recently for other purposes (Scheme I). The alternative routes shown are roughly comparable in facility and in overall yield. The requisite 1-indanones were prepared as shown in Scheme II. The homophthalic acids were converted to their anhydrides in refluxing acetyl chloride; in the case of **1e**, a mixture of acid and anhydride was obtained directly from peracetic acid oxidation of the precursor indandione and, in that of **1f**, the anhydride was the sole product of oxidation.

Homophthalic Acid–Anhydride Equilibria. For the parent compound and its simpler homologues (**1a–d**), the equilibrium content of acid anhydride in highly aqueous media is too low to permit quantitative study; accordingly, equilibrium data for the entire series were measured (at 28.5 °C) in pure acetonitrile (containing small amounts of water) as solvent. Various strong acids (Table I) were used to accelerate cyclization of the homophthalic acid or hydrolysis of the corresponding anhydride, equivalent results being obtained from either direction. Low concentrations of water, already present or added to reagent acids,

Scheme II

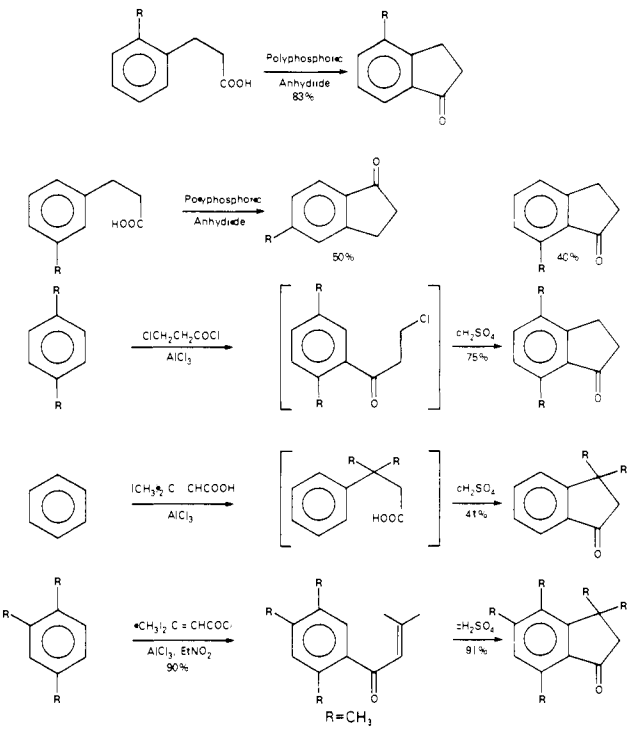

provided a range of equilibrium anhydride concentrations. Spectral analysis was performed at both 240–245 and 290–300 nm, with similar results. The representative data in Table I show, appropriately, that K_{eq} is independent of the nature of the catalyst acid and that the basic relationship, $K_{eq} = [\text{anhydride}][H_2O]/[\text{acid}]$, is followed throughout the series. As had already been observed for lactone formation,[1,3,4] anhydride content at equilibrium increases progressively with increasing alkyl substitution or conformational restriction; assuming that the cyclic anhydrides vary little in free energy content (see Discussion), the results in Table I indicate **1f** to be ca. 4.9 kcal/mol higher in energy than **1a**.

Kinetics of Ring Closure. Rates of anhydride formation, at 28.5 °C in solvent acetonitrile, were followed in the presence of nine catalyst acids ranging in strength from perchloric to acetic acid. Although perchloric acid is far stronger than necessary to achieve conveniently measurable cyclization rates for **1e** or **1f**, it is only weakly effective for **1b–d**. Cyclization of **1a** could not be observed under any conditions tried, except upon addition of acetic anhydride as an energy source. In early runs with less reactive hom-

(11) Reepmeyer, J. C.; Kikugawa, Y.; Cohen, L. A., manuscripts in preparation.

Table II. Typical Rate Constants for Cyclization of Homophthalic Acids[a]

compd	medium	k'^{tot}_{obsd},[b] min^{-1}	2, %	k^{tot}_{obsd},[c] min^{-1}	k_1, M^{-1} min^{-1}	log k_1
1a	0.12 M $HClO_4$	3.16×10^{-2} [d]	0.85	2.69×10^{-4}	2.24×10^{-3}	−2.65
1b	0.12 M $HClO_4$	2.62×10^{-2}	2	5.24×10^{-4}	4.37×10^{-3}	−2.36
	0.20 M CH_3SO_3H	1.94×10^{-3}	21	4.07×10^{-4}	2.04×10^{-3}	−2.69
1c	0.12 M $HClO_4$	3.36×10^{-2}	16	5.38×10^{-3}	4.48×10^{-2}	−1.35
	0.20 M CH_3SO_3H	2.78×10^{-3}	69	1.92×10^{-3}	9.59×10^{-3}	−2.02
1d	0.08 M $HClO_4$	3.89×10^{-2}	24	9.34×10^{-3}	0.117	−0.93
	0.20 M CH_3SO_3H	4.54×10^{-3}	71	3.22×10^{-3}	1.61×10^{-2}	−1.79
	0.73 M CF_3COOH	2.82×10^{-3}	41	1.16×10^{-3}	1.59×10^{-3}	−2.80
1e	$HClO_4$	(see Figure 1A)			148	2.17
	CH_3SO_3H	(see Figure 1B)			2.94	0.47
	0.73 M CF_3COOH	4.31×10^{-2}	89	3.83×10^{-2}	5.25×10^{-2}	−1.28
	0.42 M HCF_2COOH	4.17×10^{-3}	91	3.80×10^{-3}	9.04×10^{-3}	−2.04
1f	1.0 M $HClO_4$[e]	(see Figure 1A and Table III)			1050	3.02
	1.0 M CH_3SO_3H[e]	(see Figure 1B and Table III)			11.5	1.06

[a] At 28.5 °C in acetonitrile. [b] Values given are averages of three or more runs in each medium. [c] (k'^{tot}_{obsd}) (fraction 2). [d] Calculated from K_{app} and k_{obsd} for hydrolysis of 2a in the same medium. [e] Extrapolated from data at lower acid concentrations.

Table III. Rate Constants for Cyclization of 1f[a]

catalyst	catalyst pK-(H_2O)	catalyst pK^s-(H_2O)[b]	q/p[b]	k_1,[c] M^{-1} min^{-1}	$K_T k_4$,[d,e] M^{-1} min^{-1}	k^B_{calcd},[f] min^{-1}	k^{tot}_{obsd},[g] min^{-1}	$K_T k_s$,[h] M^{-1} min^{-1}
$HClO_4$	−4.35	−4.95	4/1	1050	(0.174	6.22×10^{-3}	1050	
CH_3SO_3H	−2.00	−2.48	3/1	11.5	(6.46×10^{-2})	5.87×10^{-3}	11.5	
CF_3COOH	0.23	−0.07	2/1	(0.163)	(2.57×10^{-2})	5.16×10^{-3}	0.168	1.89×10^{-3}
HCF_2COOH	−1.24	0.94	2/1	(2.69×10^{-2})	1.74×10^{-2})	4.71×10^{-3}	3.14×10^{-2}	
HC≡C COOH	1.84	1.54	2/1	(9.12×10^{-3})	1.38×10^{-2}	4.40×10^{-3}	1.30×10^{-2}	
$NCCH_2COOH$	2.43	2.13	2/1	(3.10×10^{-3})	1.11×10^{-2}	4.07×10^{-3}	7.25×10^{-3}	2.24×10^{-2}
$ClCH_2COOH$	2.86	2.56	2/1	(1.44×10^{-3})	9.12×10^{-3}	3.78×10^{-3}	5.41×10^{-3}	4.00×10^{-2}
CH_3OCH_2COOH	3.53	3.23	2/1	(4.36×10^{-4})	7.10×10^{-3}	3.83×10^{-3}	3.83×10^{-3}	8.10×10^{-2}
CH_3COOH	4.76	4.46	2/1	(4.68×10^{-5})	4.36×10^{-3}	2.60×10^{-3}	2.65×10^{-3}	4.34×10^{-1}
$CF_3CO_2^-$·HA	3.50	2.90	4/1				4.36×10^{-3}	
$ClCH_2CO_2^-$·HA	5.71	5.11	4/1				2.24×10^{-3}	
$CH_3OCH_2CO_2^-$·HA	6.48	5.88	4/1				1.82×10^{-3}	

[a] At 28.5 °C in acetonitrile. [b] pK values (see Table IV for sources) have been statistically corrected (pK^s), using the q/p values shown; see ref 25, Chapter 10. [c] Values in parentheses were obtained by extrapolation of slope A in Figure 5. [d] Values derived from the slopes of reciprocal plots (eq 4 and 6; see Figure 6 for examples). [e] Values in parentheses obtained by extrapolation of slope B in Figure 5. [f] Calculated from eq 4 for 1 M catalyst. [g] For 1 M catalyst; for the stronger acids, these values are extrapolations from rate data at lower concentrations. [h] Derived from the slopes of reciprocal plots according to eq 8 and 4.

ophthalic acids, anhydrous magnesium perchlorate was added in an effort to drive cyclization further to completion by removal of water. This goal was achieved, but the drying agent also increased rates of cyclization significantly, possibly through formation of perchloric acid;[12] the results proved confusing and unreproducible and this approach was abandoned. The catalytic efficiency of perchloric acid in acetonitrile decreases gradually with aging,[13] and it was found necessary to prepare stock solutions daily in order to achieve good reproducibility. Initial substrate concentrations were usually 0.006 M, while the catalyst concentrations necessary for practical rate measurement varied widely. Kinetics were followed in the same wavelength regions given above for equilibria for 2–3 half-lives. The first-order rate law was obeyed in all cases, with most correlation coefficients greater than 0.999. All reported rate constants are averages of three or more runs, with a range rarely exceeding 5%. Experimental rate constants (K'^{tot}_{obsd}) have been adjusted for equilibria, which were determined under the same conditions as the kinetic runs; the adjusted values are expressed as k^{tot}_{obsd}.

Strong Acid Catalysis (Path A). In the presence of acids such as perchloric, methanesulfonic, and trifluoroacetic, rate constants for cyclization of **1b–f** in acetonitrile are linear functions of acid concentration (eq 1), at least within the range of convenient

$$k^{tot}_{obsd} = k_1[HA] + k_0 \quad (1)$$

measurement. Typical concentration dependence plots are shown in Figure 1 and values of k_1 are given in Table II (column 6). The intercept values, k_0, which may result from spontaneous cyclization (intermolecular general acid catalysis) and from catalysis by other substrate molecules, are negligibly small at the concentrations used for UV kinetic analysis. The latter (intermolecular) contribution, however, increases with concentration; IR and NMR spectra, for **1e** and **1f**, show time- and concentration-dependent anhydride formation in inert solvents (this complication in the recording of spectra can be minimized by the use of fairly dilute, fresh solutions).

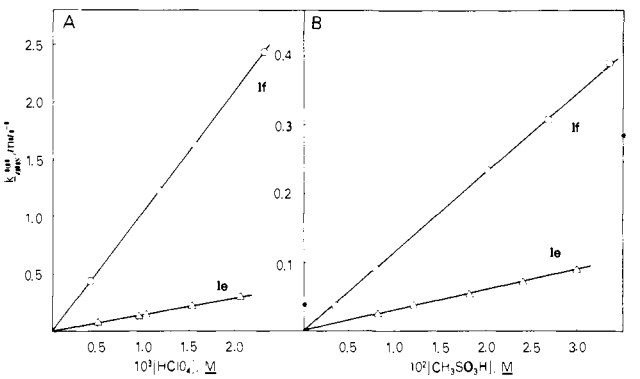

Figure 1. Dependence of k^{tot}_{obsd} for cyclization of **1e** and **1f** in acetonitrile at 28.5 °C on the concentrations of perchloric acid (A) and methanesulfonic acid (B).

The k_1 values in Table II and the catalyst pK(H_2O) values in Table III (statistically corrected values are designated pK^s)[1] were used to construct Brønsted plots (Figure 2). For **1b–d**, catalysis

(12) Greenhow, E. J.; Parry-Jones, R. L. *Fresenius Z. Anal. Chem.* **1973**, *264*, 381.
(13) Kolthoff, I. M.; Bruckenstein, S.; Chantooni, M. K. *J. Am. Chem. Soc.* **1971**, *83*, 3927.

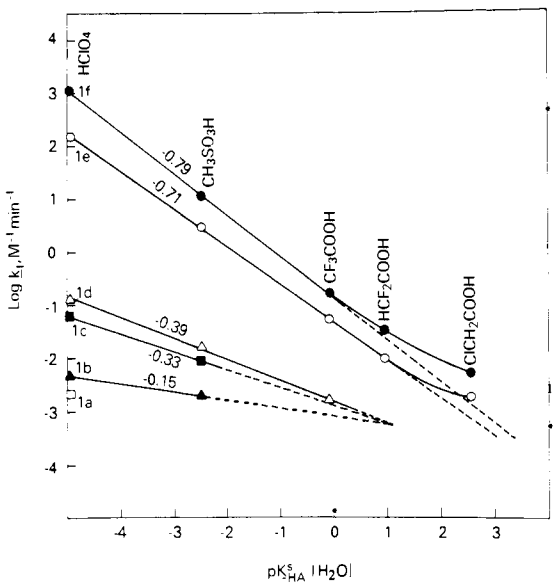

Figure 2. Brønsted plots for cyclization of homophthalic acids with various acid catalysts (aqueous pK values are statistically corrected).

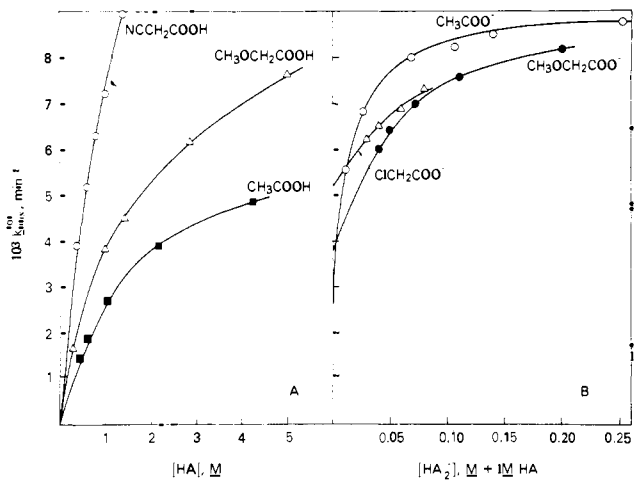

Figure 3. Dependence of k_{obsd}^{tot} for cyclization of **1f** on the concentrations of various carboxylic acid catalysts (A), and on the concentrations of homoconjugate anions (HA_2^-) in the presence of 1 M HA (B).

by acids weaker than those listed in Table II was barely detectable, and the data are considered unreliable. For **1f**, the principal compound in this study, the linear Brønsted slope is defined by eq 2. As shown below, pK values in acetonitrile [pK(AN)] have

$$\log k_1 = -0.79pK^s - 0.84 \qquad (2)$$

a reasonably linear relationship to those in water over the entire pK range examined; since Brønsted slopes normally refer to aqueous media, we chose to use pK(H_2O) values in our plots for the sake of some comparability with other data.[14]

Weak Acid Catalysis (Path B). In the presence of less acidic carboxylic acids, readily measurable rates of cyclization were observed only for **1e** and **1f**. With these catalysts, the dependence of k_{obsd}^{tot} on [HA] is *not* linear, the degree of curvature becoming more pronounced as the pK of the catalyst acid increases (Figure 3A). Such results suggest a change in rate-limiting step dependent on catalyst concentration, a phenomenon sometimes observed in reactions involving tetrahedral intermediates.[15] In fact, curvature in catalyst dilution plots provides strong evidence for the very existence of a transient, tetrahedral intermediate. Assuming that

(14) Bell, R. P. *Adv. Catal.* **1952**, *4*, 162.
(15) Jencks, W. P. "Catalysis in Chemistry and Enzymology"; McGraw-Hill: New York, 1969; pp 477–480.

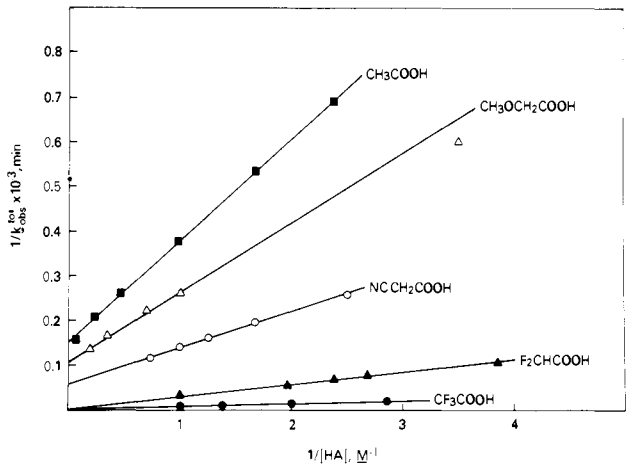

Figure 4. Reciprocal plots (eq 4) of kinetic data (k_{obsd}^{tot}) for weak acid catalysis of cyclization of **1f** (including the data shown in Figure 3A).

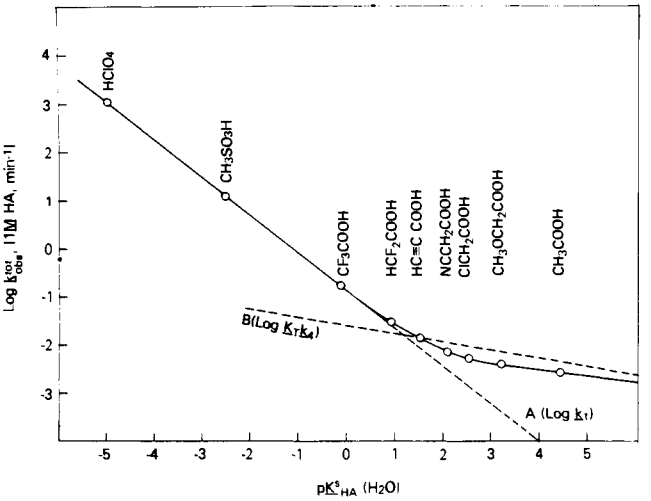

Figure 5. Modified Brønsted plot for cyclization of **1f** with various acid catalysts. The circles are based on experimental values of k_{obsd}^{tot} for 1 M catalyst acid or, for the stronger acids, on values obtained by extrapolation to this concentration. Slope A (solid and dashed) is the calculated slope for catalysis by path A (eq 2); slope B is the calculated slope for catalysis by path B (eq 7). The solid curve = log ($k_{calcd}^A + k_{calcd}^B$); $k_{calcd}^A = k_1$ (Table III, column 5), and values of k_{calcd}^B are given in Table III, column 7.

the acid catalyzes breakdown of the tetrahedral intermediate (eq 3),[3] the steady-state kinetic treatment leads to eq 4 and the ex-

$$\mathbf{1f} \underset{k_3}{\overset{k_2}{\rightleftharpoons}} \mathrm{T} \xrightarrow{k_4[HA]} \mathbf{2f} \qquad (3)$$

$$k_{obsd}^{tot} = \frac{k_2k_4[HA]}{k_3 + k_4[HA]} \text{ and } \frac{1}{k_{obsd}^{tot}} = \frac{1}{k_2} + \frac{k_3}{k_2k_4}\left(\frac{1}{[HA]}\right) \qquad (4)$$

pectation of linearity in plots of $1/k_{obsd}^{tot}$ vs. $1/[HA]$. Furthermore eq 3 and 4 require that the intercept value, $1/k_2$, be the same for all acids used as catalysts. It is evident from Figure 4, that, while the condition of linearity in the reciprocal plots is met quite well, the intercepts do *not* coincide.

We then considered the possibility of two concurrent and independent pathways for anhydride formation (eq 5), with con-

$$k_{obsd}^{tot} = k_{obsd}^A + k_{obsd}^B \qquad (5)$$

tributions to k_{obsd}^{tot} following both eq 1 (path A) and eq 4 (path B). For weak acids, the contribution to k_{obsd}^{tot} due to path A should be relatively small and cannot be evaluated directly from kinetic data. Extrapolation of slope A in Figure 5 (the expanded Brønsted plot for **1f**) provides predicted values of log k_1 (from eq 2) for the weaker acid catalysts (Table III, column 5), assuming that linearity in the Brønsted relationship is maintained for the entire

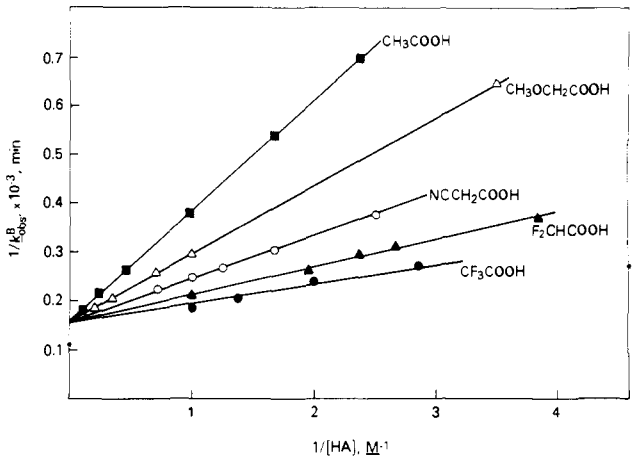

Figure 6. Reciprocal plots (eq 4) of kinetic data (k^B_{obsd}) for weak acid catalysts, according to eq 6 and 4.

pK range. Predicted values of k^A_{obsd} were then calculated (eq 1) for each concentration of a given catalyst acid. Subtraction of the latter values from k^{tot}_{obsd} (eq 5) provided values for k^B_{obsd}; reciprocal plots ($1/k^B_{obsd}$ vs. $1/[HA]$, Figure 6) now confirm the coincidence of values of $1/k_2$ and obedience to eq 4 (with k^B_{obsd} replacing k^{tot}_{obsd}). The intercepts of Figure 6 provide a value of $k_2 = 6.45 \times 10^{-3}$ min^{-1}; the slopes of the same plots correspond to $k_3/(k_2k_4)$ in eq 4. This factor cannot be resolved into its component rate constants, but can be simplified to K_Tk_4 (eq 6),

$$1/\text{slope} = k_2k_4/k_3 = K_Tk_4 \quad (6)$$

in which K_T is the equilibrium constant for "spontaneous" formation of the tetrahedral intermediate. In Table III are listed, for **1f**, the values of k_1 and K_Tk_4 for all the acid catalysts used in this study.

The values of K_Tk_4 were then used to construct a Brønsted plot for general acid catalysis by path B (Figure 5, slope B), defined by eq 7. Extrapolation of this plot to the stronger acid region

$$\log (K_Tk_4) = -0.17pK^s - 1.60 \quad (7)$$

provides the very small values of log (K_Tk_4) for the more acidic catalysts. From these specific rate constants, values of k^A_{calcd} (numerically equal to k_1) and k^B_{calcd} were obtained for 1 M HA (Table III, columns 5 and 7, respectively). It is readily seen that, for strong acids, k^{tot} is derived overwhelmingly from k^A; consequently, the dilution plots (Figures 1) show no significant curvature and $k^{tot}_{obsd} \simeq k^A_{obsd}$. Conversely, for the very weak acids, k^{tot}_{obsd} is derived mainly from k^B_{obsd} while, for catalyst acids of intermediate strength (pK 1–3), both pathways make significant contributions. The calculated values (for 1 M HA) of k^{tot} (Table III, sum of columns 5 and 7) were used to construct the solid line in Figure 5; the open circles correspond to the experimental values of k^{tot}_{obsd} for 1 M acid (Table III, column 8). The experimental points for perchloric and methanesulfonic acids are based on extrapolation to 1 M catalyst from kinetic data at lower concentrations (the range of practical measurement). The *linear* summation plot, which should result from addition of slopes A and B of Figure 5 (eq 2 and 7), would be experimentally attainable only at extremely low concentrations of HA (before the curvatures of Figure 3 become significant). As a result of dual pathways with different rate laws, the Brønsted plot based on k^{tot} (solid line, Figure 5) shows the normal property of concentration independence for strong acids, but concentration dependence for weak catalyst acids.

Base Catalysis (Path B′). Since significant general base catalysis had been observed in lactonizations,[1,3] it seemed reasonable to expect the same phenomenon in anhydride formation. No catalysis of the cyclization of **1f** could be detected with the homoconjugate salt, (n-Bu)$_4$N$^+$ OAc$^-$·HOAc,[16] in acetonitrile;

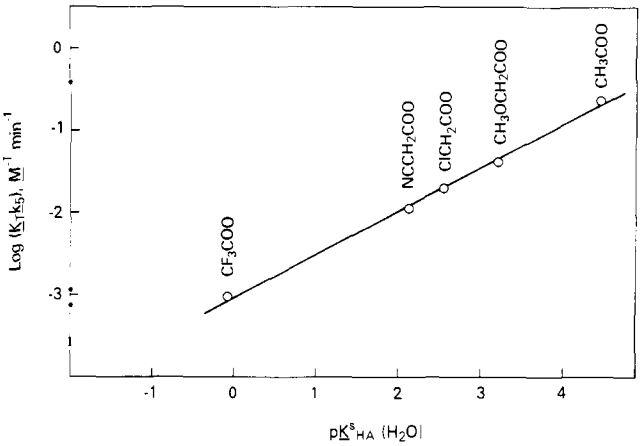

Figure 7. Brønsted plot for cyclization of **1f** with base catalysis by various homoconjugate anions.

however, when low concentrations of the homoconjugate salt were added to larger concentrations of acetic acid, the values of k^{tot}_{obsd} were increased significantly above those due to the acid alone (Figure 3B). At very low concentrations (10^{-2} to 10^{-3} M), homoconjugate acetate ion (HAc_2^-) is 50- to 100-fold as effective a catalyst as is acetic acid at the same concentration (Figure 3). Similar results were obtained with the homoconjugate salts (HA_2^-) of other weak acids in the presence of the corresponding acid. Such enhancements cannot be due simply to an increase in ionic strength, since (n-Bu)$_4$N$^+$Cl$^-$ had no detectable effect on cyclization rate, with or without added catalyst acid.

After substraction from k^{tot}_{obsd} of the contribution due to acid catalysis at each concentration, plots of the residual k_{obsd} vs. $[HA_2^-]$ showed curvatures similar to those observed for acid catalysis. These results suggested the existence of a path B′, analogous to path B, which follows eq 8 and a steady-state rate equation parallel

$$\mathbf{1f} \underset{k_3}{\overset{k_2}{\rightleftharpoons}} \text{T} \xrightarrow{k_5[HA_2^-]} \mathbf{2f} \quad (8)$$

to eq 4. Indeed, plots of $1/k_{obsd}$ vs. $1/[HA_2^-]$ are linear, give a common intercept value for several homoconjugate bases, and this intercept value ($1/k_2$) is *identical* with that obtained for acid catalysis (path B). These results are required if eq 3, 4, and 8 truly describe the events of paths B and B′.

The components of a homoconjugate carboxylate ion are tightly bound by hydrogen and ion–dipole bonding. For example, the dissociation constant ($K^d_{HA_2^-}$) in acetonitrile for the acetate complex is 2.13×10^{-4};[17] although similar data are unavailable for substituted acetic acids, a series of benzoic acid homoconjugates[17] shows relatively small changes in dissociation constants (in acetonitrile) over a wide range of benzoic acid pK(AN) values. Further, a roughly linear correlation exists between pK_{HA}(AN) and log $K^d_{HA_2^-}$ for this series, the degree of dissociation of HA_2^- decreasing slightly as the acid strength of HA increases. Our kinetic results show that k^{tot}_{obsd} for cyclization of **1f** in the presence of 0.14 M trifluoroacetic acid and 0.14 M homoconjugate salt is only slightly larger than that with the acid alone. Had there been any significant dissociation of the homoconjugate salt, a sizable increase in k^{tot}_{obsd} should have been observed. In mixtures of HA and HA_2^-, the catalytic contribution of HA_2^- is most effective with the acetate ion, falling off rapidly with decreasing pK of HA and becoming barely detectable at trifluoroacetate (Table III). The trend in catalytic efficiency suggests that the phenomenon is truly base catalysis; a Brønsted plot of log $k^{B'}_{obsd}$ vs. pK^s_{HA}(H_2O) provides a β value $\simeq$0.50 (Figure 7). This value implies that proton transfer from the tetrahedral intermediate to HA_2^- is about half complete at the transition state.

We have already noted that the homoconjugate of acetate ion shows no measurable catalytic activity in the absence of acetic

(16) The simple quaternary salts were found so hygroscopic and difficult to purify that the more manageable acid salts (homoconjugates) were used in these studies.

(17) Chantooni, M. K., Jr.; Kolthoff, I. M. *J. Am. Chem. Soc.* **1970**, *92*, 7025.

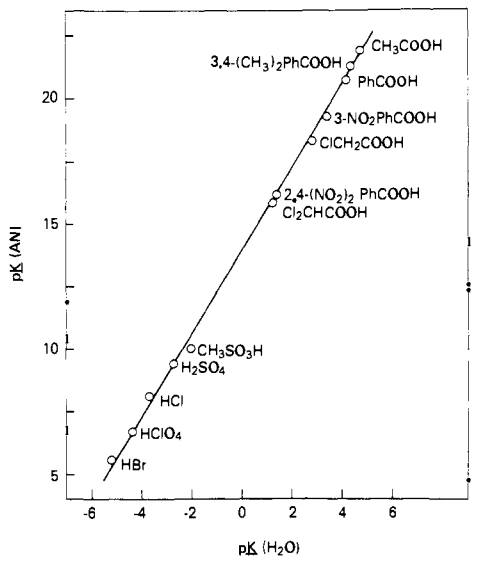

Figure 8. Correlation of values of pK(H_2O) with pK(acetonitrile), based on data given in table IV.

acid. Surprisingly, however, the homoconjugate anions of stronger carboxylic acids do exhibit weak catalysis by themselves, with k_{obsd}^{tot} now *decreasing* with an increase in pK_{HA} (Table III, column 8). The values of k_{obsd} are much smaller than those expected for comparable concentrations of HA or of HA + HA_2^-, and the results are best interpreted by considering HA_2^- to function as a weak acid catalyst. From the Brønsted slopes (eq 2 and 7) and values of k_{obsd}^{tot}, "apparent" pK(H_2O) values can be calculated for $HA_2^- \rightleftharpoons H^+ + 2A^-$ (Table III). These pK values are ca. 3 units higher than those for the corresponding HA's, and, interestingly, the two sets show a linear relationship (based on three points).

pK(H_2O) - pK(AN) Correlations. In the Brønsted plots (Figures 2, 5, and 7), we have used pK(H_2O) values for the catalyst acids for the sake of consistency with common practice.[14] This substitution is permissible because a reasonably linear relationship between pK values in water and in acetonitrile can be demonstrated over the entire pK range of this study (Figure 8). Such a relationship had previously been shown for a series of substituted benzoic acids.[18] The degree of fit (r = 0.9993) for a single correlation including aliphatic acids, sulfonic acids, and even stronger inorganic acids is surprisingly good, considering the magnitude of error in estimates of "apparent" pK for strong acids in water and in acetonitrile. The pK values (and their sources) used to establish the regression line (eq 9) of Figure 8 are given

$$pK(AN) = 1.64[pK(H_2O)] + 13.87 \quad (9)$$

in Table IV. For certain strong acids, the best fit in the correlation was realized by use of "apparent" pK(H_2O) values derived, not from physical or spectral data, but from leaving group abilities;[5,19] for perchloric acid, for example, the latter approach gives a value of -4.35, which may be compared with the two reported estimates, -7.7[20a] and -1.58.[20b] The relatively high basicity of water has a leveling effect on strong acids, leading to essentially complete dissociation in most cases. In the much more weakly basic solvent, acetonitrile, marked differences in acid strength can be observed in conductivity measurements, as well as in catalytic efficiency; thus, kinetic studies in such solvents permit a roughly quantitative ranking of strong acids.

Activation Parameters. The effect of temperature on k_{obsd}^{tot} for cyclization of **1f** was determined in the presence of 0.14 M trifluoroacetic acid or 1 M acetic acid. At these concentrations, ca 95% of k_{obsd}^{tot} is due to path A for the stronger acid and to path B for the weaker acid; thus, the results should be reasonably characteristic of the separate pathways. Over the temperature range examined (28–42 °C), variation in the pK of carboxylic acids is small enough to be neglected.[21] For trifluoroacetic acid catalysis, E_a = 14.7, $\Delta H^{\ddagger}$ = 14.1, and $\Delta F^{\ddagger}$ = 21.1 kcal/mol; $\Delta S^{\ddagger}$ = -23.5 eu. For acetic acid catalysis, E_a = 15.0, $\Delta H^{\ddagger}$ = 14.4, and $\Delta F^{\ddagger}$ = 23.5 kcal/mol; $\Delta S^{\ddagger}$ = -30.7 eu. All calculations were based on T = 298 K and 1 M catalyst; plots of log k vs. $1/T$ were based on four points and gave excellent linearity (r > 0.999).

Table IV. pK(H_2O) and pK(AN) Values (Used in Figure 8)

acid	pK(H_2O)	pK(AN)
CH_3COOH	4.76[a]	21.9[b]
3,4-$(CH_3)_2$PhCOOH	4.50[c]	21.2[d]
PhCOOH	4.20[a]	20.0[b]
3-NO_2PhCOOH	3.45[a]	19.3[d]
$ClCH_2COOH$	2.86[a]	18.3[b]
2,4-$(NO_2)_2$PhCOOH	1.42[e]	16.2[d]
$Cl_2CHCOOH$	1.29[a]	15.8[f]
CH_3SO_3H	-2.00[g]	10.0[h]
H_2SO_4	-2.70[g]	9.4[b]
HCl	-3.70[i]	8.1[j]
$HClO_4$	-4.35[g]	6.7[b]
HBr	-5.20[i]	5.5[j]

[a] Brown, H. C.; McDaniel, D. H.; Hafliger, O. In "Determination of Organic Structures by Physical Methods"; Braude, E. A., Nachod, F. C., Eds.; Academic Press: New York, 1955; Vol. I, Chapter 14. [b] Desbarres, J. *Bull. Soc. Chim. Fr.* **1962**, 2103. The reported values were increased by 4.8 pK units to bring them to the same scale used by other investigators. [c] Luning, B. *Acta Chim. Scand.* **1960**, *14*, 321. [d] Reference 18b. [e] Dippy, J. F. J.; Hawkins, B. D.; Smith, B. V. *J. Chem. Soc.* **1964**, 154. [f] Chantooni, M. K., Jr.; Kolthoff; I. M. *J. Phys. Chem.* **1975**, *79*, 1176. [g] Derived from leaving ability data (ref 5 and 19, and work in progress). [h] Kolthoff, I. M.; Chantooni, M. K., Jr. *J. Am. Chem. Soc.* **1965**, *87*, 4428. [i] Reference 20a. [j] Reference 13.

Isotope Effects. Kinetics of ring closure of **1f** in acetonitrile were measured in the presence of 0.14 M CF_3COOD or 1 M CH_3COOD. For the stronger acid, k_{obsd}^{tot}(DA) = 1.08 × 10^{-2} min^{-1} vs. 2.22 × 10^{-2} min^{-1} for HA. For the weaker acid, k_{obsd}^{tot}(DA) = 5.60 × 10^{-4} min^{-1} vs. 2.65 × 10^{-3} min^{-1} for HA. For both acids, the rate constants include contributions from paths A and B, which should be separated before accurate k^H/k^D ratios can be calculated. Hypothetical contributions to k_{obsd}^{tot}, without consideration of kinetic isotope effects, were calculated by use of eq 2 and 1 for path A, and eq 7 and 4 for path B. These results were used to solve the simultaneous eq 10a and 10b, in which A_D and B_D

$$CF_3COOD: \quad 10^4 k_{obsd}^{tot} = 100.6/A_D + 20.52/B_D = 108\ (min^{-1}) \quad (10a)$$

$$CH_3COOD: \quad 10^4 k_{obsd}^{tot} = 0.174/A_D + 23.12/B_D = 5.60\ (min^{-1}) \quad (10b)$$

are the isotope effects for the respective pathways:[22] A_D = 0.98; B_D = 4.26. If the contribution due to the minor pathway is neglected for each case, as was done in calculating activation parameters, the change in isotope ratios is relatively small: A_D, 0.93; B_D; 4.13.

The calculated values of k_{obsd} for the respective pathways in eq 10a and 10b can be obtained from eq 2 and 7 only if pK(H_2O) values are known for the deuterated acid catalysts. Since such values cannot be obtained by direct measurement, they were estimated from the O–H and O–D stretching frequencies of the respective acids, as dilute solutions in acetonitrile: for CH_3CO-OH(D), $\bar{\nu}_{OH}$ = 3276 and $\bar{\nu}_{OD}$ = 2437 cm^{-1};[23] for CF_3COOH(D),

(18) (a) Miron, R. R.; Hercules, D. M. *Anal. Chem.* **1961**, *33*, 1770. (b) Kolthoff, I. M.; Chantooni, M. K., Jr. *J. Am. Chem. Soc.* **1971**, *93*, 3843.
(19) Lohmann, K. H. Ph.D. Thesis, Massachusetts Institute of Technology, Cambridge, Mass., 1959. Thorton, E. R. "Solvolysis Mechanisms"; Ronald Press: New York, 1964; p 164.
(20) (a) Bessière, J. *Anal. Chim. Acta* **1970**, *52*, 55. (b) Hood, G. C.; Redlich, O.; Reilly, C. A. *J. Chem. Phys.* **1954**, *22*, 2067.
(21) Izatt, R. M.; Christensen, J. J. "Handbook of Biochemistry"; Sober, H. A., Ed.; Chemical Rubber Co.: Cleveland, Ohio, 1968; pp J-49–J-139.
(22) These ratios also include the kinetic effects of deuteration of **1f**, which effects are presumed to be relatively small.
(23) Bellamy, L. J.; Osborn, A. R.; Pace, R. J. *J. Chem. Soc.* **1963**, 3749.

Table V. Kinetics of Homophthalic Anhydride Hydrolysis[a]

compd	k^{aq}_{obsd}[b]	k_{obsd}[c]	$\bar{\nu}_{C=O}(CHCl_3)$, cm^{-1}
2a	1.06	0.0314	1805, 1760
2d	0.55	0.0616	1800, 1755
2e	1.12	6.50	1790, 1750
2f	0.27	3.90[d]	1785, 1740

[a] Min^{-1} at 28.5 °C. [b] In 0.1 N aqueous HCl; hydrolysis is complete for all compounds. [c] In 0.12 N $HClO_4$ in acetonitrile (0.42 M H_2O), corrected for equilibrium. [d] Estimated from k_{obsd}(cyclization) and K_{app}.

$\bar{\nu}_{OH}$ = 3059 and $\bar{\nu}_{OD}$ = 3212 cm^{-1}. From these values,[24] and eq 11 and 12,[25] K_H/K_D ratios in acetonitrile were calculated for the

$$\Delta E_0 = \tfrac{1}{2}h(\nu_{OH} - \nu_{OD}) \quad (h = \text{Boltzmann's constant}) \quad (11)$$

$$K_H/K_D \simeq \exp(\Delta E_0/kT) \quad (k = \text{Planck's constant}) \quad (12)$$

two acids. Values of $pK(H_2O)$ for the deuterated acids were than obtained from eq 9: CH_3COOD, 5.26; CF_3COOD, 0.68.

Homophthalic Anhydride Hydrolysis. The kinetics of ring opening of four homophthalic anhydrides were followed in 0.1 N aqueous hydrochloric acid; in this medium, ring opening is complete for each compound. As seen from Table V (column 2), the introduction of methyl groups, adjacent to either or both carbonyls, has relatively little effect on the ease of ring opening. Rate constants for hydrolysis of five-membered cyclic anhydrides show almost no pH dependence from pH 5.5 to 0.2 N hydrochloric acid,[26] and the mechanism apparently involves nucleophilic attack by water alone. We have not examined the effect of acid concentration in the hydrolysis of homophthalic anhydrides but assume the same mechanism to be applicable. The rate constants of Table V (**2d**/**2a** and **2f**/**2e**), together with σ^0 values for the aromatic methyl groups,[27] give a ρ value for solvolysis = 1.25. This value is fairly close to that (ρ = 1.12) for alkaline hydrolysis of ethyl phenylacetates in aqueous ethanol,[27] suggesting that the variations in k^{aq}_{obsd} in Table V are due almost entirely to the electronic effects of the methyl groups. This analysis assumes that attack by water occurs selectively at the aliphatic carbonyl group in the anhydride; the assumption is supported by the results of methanolysis (see Discussion).

Hydrolysis of **2a** in acetonitrile (0.12 M $HClO_4$, 0.42 M H_2O) is slower by a factor of 34 than in water alone (Table V, column 3). This retardation was presumed due to the low water content of the medium; however, in the presence of 3 to 6 M water in acetonitrile, k_{hyd} for **2a** is reduced even further (0.016 min^{-1}), increasing slowly as additional water is added. These results suggest a change in mechanism of hydrolysis in going from almost pure acetonitrile to highly aqueous media. Under the nonaqueous hydrolysis conditions, the effects of methyl groups (Table V, column 3) on k_{hyd} do not follow the pattern seen for hydrolysis in water, showing *facilitation* rather than the electronic or steric retardation expected for pathways involving tetrahedral intermediates.

Discussion

We have found no previous reports on the mechanisms of anhydride formation, although a number of studies of anhydride hydrolysis are available.[28] Pathways for cyclization undoubtedly reflect those for hydrolysis, and are probably analogous to the more common pathways for ester and lactone formation.[3,28c,29] In all reactions involving tetrahedral intermediates, it is generally difficult to identify the rate-limiting step.[30] Rate-determining formation or breakdown of the tetrahedral intermediate *may* depend on whether the reaction is inter- or intramolecular;[27] on pH, solvent polarity, or catalyst concentration;[30] on the nature and charge state of the leaving group;[30] and, in intramolecular reactions, on the degree of assistance by other substituents. The formation of homophthalic anhydrides proved to be even more complex mechanistically, in that the experimental results are best explained on the basis of at least two simultaneous pathways, their relative contributions being governed by the strength of the catalyst acid and the substitution pattern in the diacid. General acid catalysis of lactonization, covering the pK range −2 to +8 (10 units), gave no evidence of curvature either in catalyst dilution plots or in Brønsted slopes.[1,3] In the present study, data for **1f** were obtained for the pK range −5 to +5 (10 units); the curvatures found in the catalyst dilution plots (Figure 3) and in the Brønsted plots (Figures 2 and 5) are very clear and are far beyond the range of experimental error. The catalyst dilution plots in acetonitrile involve neither buffers nor constant pH, and use of the terms "general acid" or "general base" may be unjustified in the present study.

Scheme III

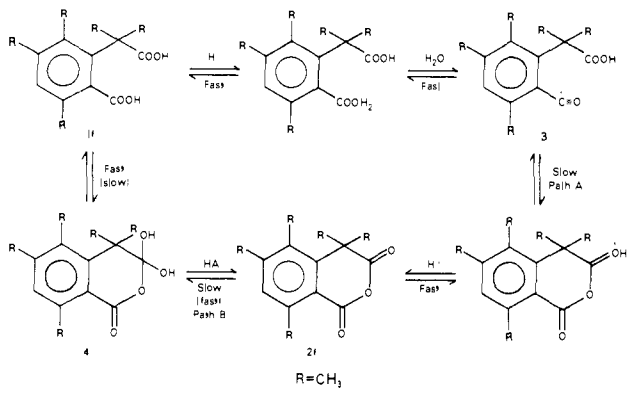

Our analysis of the kinetic results began with the assumption of two concurrent and independent pathways, A and B. For strong acid catalysis, k^{tot}_{obsd} is a linear function of [HA], $\Delta S^{\ddagger}$ = −23 eu, $k_H/k_D \simeq 1$, and Brønsted α = −0.79. In the absence of a significant isotope effect, a Brønsted slope of ~1 is expected.[31] Since both our isotope effect and Brønsted slope are based on data involving a nonaqueous medium, we do not anticipate a full correspondence with behavior in aqueous systems;[25] nevertheless, these values do suggest that proton transfer to **1f** is already well advanced in the transition state, and we tentatively propose mechanism A (Scheme III) for this pathway. Acylium ion (**3**) formation should be favored by the crowding effect of two alkyl substituents ortho to the aromatic carboxylic group,[28,32] and even by one "tert-butyl" group (as in **1e**). Further support for path A is found in the data for anhydride hydrolysis in wet acetonitrile (Table V, column 3) in that steric crowding (as in **2e**) and/or hyperconjugative stabilization (as in **2f**) *facilitate*, rather than retard ring opening. Kinetics of hydrolysis of **2a** also indicate a change in mechanism as the water content of solvent acetonitrile is increased, possibly reflecting a transition from path A to path B. The basicity of the C-3 carbonyl group (and its enhancement by the 4,4-dimethyl group) may also be a significant factor in determining rate constants for ring opening; the carbonyl stretching frequencies of the anhydrides (Table V, column 4) show a trend consistent with increasing carbonyl basicity.[33] The value of $\Delta S^{\ddagger}$

(24) These frequencies very probably represent monomer bands.[23] It has been shown that dissociation of carboxylic acid dimers occurs readily in acetonitrile: Reeves, L. W. *Trans. Faraday Sco.* **1959**, *55*, 1684.

(25) Bell, R. P. "The Proton in Chemistry"; Cornell University Press: Ithaca, N.Y., 1973; pp 226–230.

(26) Eberson, L. *Acta chem. Scand.* **1964**, *18*, 534, 1276. Thanassi, J. W.; Bruice, T. C. *J. Am. Chem. Soc.* **1966**, *88*, 747.

(27) Cohen, L. A.; Takahashi, S. *J. Am. Chem. Soc.* **1973**, *95*, 443.

(28) (a) Bunton, C. A.; Perry, S. G. *J. Chem. Soc.* **1960**, 3070. (b) Bunton, C. A.; Fendler, J. H.; Fuller, N. A.; Perry, S.; Rocek, J. *J. Chem. Soc.* **1965**, 6174. (c) Talbot, R. J. E. "Comprehensive Chemical Kinetics"; Bamford, C. H., Tipper, C. F. H., Eds.; Elsevier: New York, 1972; p 280.

(29) Euranto, E. K. "The Chemistry of Carboxylic Acids and Esters"; Patai, S., Ed.; Interscience: New York, 1969; Chapter 11.

(30) (a) Bender, M. L. "Mechanisms of Homogeneous Catalysis from Protons to Proteins"; Wiley-Interscience: New York, 1971; p 107. (b) Reference 15, p 467.

(31) Reference 30a, p 88.

(32) Reference 29, p 564.

(33) Colthup, N. B.; Daly, L. H.; Wiberley, S. E. "Introduction to Infrared and Raman Spectroscopy"; Academic Press: New York, 1964; Chapter 9.

for **1f** (−23 eu) seems too negative for rate-limiting acylium ion formation,[28,32] and cyclization may, therefore, be rate limiting. There appear to have been no studies on the ease of acylium ion formation from 2-*tert*-butylbenzoic acids; while acylium ion formation is considered to be rate limiting for mesitoic acid systems, the much greater crowding effect of a *tert*-butyl group could accelerate this step considerably. Since the same degree of steric crowding does not exist in **1a–d**, and since there is a sharp drop in Brønsted α between **1d** and **1e** (Figure 2), we cannot assume that the acylium ion pathway holds for all members of the series, or that dual pathways exist for **1a–d**. On the other hand, methanolysis studies with **2a** support acylium ion formation: under basic or neutral conditions, a mixture of 80% aliphatic monoester and 20% benzoic monoester is formed; with strong acid catalysis, the benzoic ester is formed exclusively. Parallel experiments could not be run with **2e** or **2f** because any monoester formed would recyclize spontaneously under acidic conditions (see Experimental Section).

Extrapolation of the Brønsted slope (Figure 5, slope A) to high pK values shows that the contribution of path A to k_{obsd}^{tot} drops sharply with decreasing catalyst acidity (Table III, column 5), permitting detection of path B. In the presence of weak carboxylic acid catalysts, k_{obsd}^{B} for **1f** gradually becomes less dependent on catalyst concentration (Figure 3A) and approaches a limiting value which is found to be identical (6.45×10^{-3} min^{-1}) for all the catalyst acids examined (Figure 6). At high catalyst concentration, breakdown of the tetrahedral intermediate apparently proceeds so rapidly that its uncatalyzed formation becomes rate limiting. An attempt to trap the tetrahedral intermediate from **1f** by reaction with diazomethane produced only the dimethyl ester of the homophthalic acid. For path B, $\Delta S^{\ddagger} = -31$ eu, $k_H/k_D = 4.3$, and Brønsted $\alpha = -0.17$. The value of α seems rather low for an isotope effect of such magnitude;[31] as discussed above for path A, expectations for aqueous media may not be totally transferable to acetonitrile. Yet, these results suggest that proton transfer to substrate has proceeded to a limited extent in the transition state and lead us to propose mechanism B (Scheme III) for the slower pathway. For mechanism B, we have shown formation of a tetrahedral intermediate involving the aliphatic carboxyl group (at C-3). This choice is based on the observations that the monoester produced by methanolysis (NaOMe) of **2f** involves attack at the C-3 carbonyl group, and that borohydride reduction of **2f** occurs at the same position. The results are somewhat surprising, since nucleophilic attack at C-3 and/or formation of the corresponding tetrahedral intermediate should be sterically retarded by the C-4 methyls; the steric effect would be expected to negate, if not surpass in importance, the somewhat greater reactivity of the aliphatic carbonyl group (relative to the benzoic carbonyl group).[34] An explanation has been offered for this unexpected selectivity in hydride reduction, based on prior complexing of the benzoic carbonyl group with the reagent.[34a] Such an explanation is not applicable to the methanolysis results, and an alternative interpretation becomes necessary.

In aqueous media, a reaction following path B would probably include water as a general base to assist in proton removal from the tetrahedral intermediate;[3] acetonitrile, however, may be too weakly basic to play the same role. In the latter case bifunctional participation by the catalyst acid can be visualized as an alternative (4). The validity of mechanism B (without regard to bifunctional

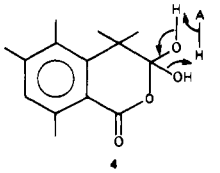

4

participation) is supported by the demonstration that base catalysis by HA_2^- follows a similar rate law (eq 9) as for acid and provides the *same* limiting value for $k_{obsd}^{B'} = k_2$. Coincidence in the values of k_2 rules out the possibility that the curvatures in Figure 3A reflect a concentration-dependent loss of catalyst activity through cyclic dimer formation. Furthermore, NMR spectra show that carboxylic acid dimers are readily dissociated in acetonitrile.[24] Base catalysis can be observed, however, only in the presence of a moderate excess of the catalyst acid. This requirement suggest that acid and base may combine to catalyze breakdown of the tetrahedral intermediate via a weak ternary complex. As an alternative explanation, the more basic HA_2^- species may render **1f** kinetically inactive by converting it to its mono- and dianion; added HA may then function as a buffering acid by maintaining **1f** largely in its neutral form. Indeed, the less basic HA_2^- species appear to function as weak acid catalysts in the absence of added HA, making the latter explanation rather difficult to rule out.

Table VI. Rate Comparisons for Cyclization of 1a-f[a]

compd	k'_{obsd}	2,[b] %	k_{obsd}[c]	k_{rel}	$t_{1/2}$,[d] min
1a[e]	3.16×10^{-2}	0.85	2.69×10^{-4}	1	
1b	2.50×10^{-2}	2	5.24×10^{-4}	2	28
1c	3.36×10^{-2}	16	5.38×10^{-3}	20	21
1d	7.78×10^{-2}	18	1.40×10^{-2}	52	9
1e	24.67	72	17.76	6.6×10^{4}	0.028
1f	129.9	97	126.0	4.7×10^{5}	0.005

[a] All data in min^{-1} for 0.12 M $HClO_4$ in acetonitrile at 28.5 °C. [b] Per cent anhydride at equilibrium. [c] Corrected for equilibrium. [d] Half-time to reach equilibrium (based on k_{obsd}). [e] Rate constants calculated from k_{obsd} for hydrolysis and K_{app} in the same medium.

The Brønsted plot for **1e** (Figure 2) shows curvature beginning at about the same pK value as for **1f**; presumably, the same duality of pathways exists for this homophthalic acid as well, but catalyst acids weaker than chloroacetic were not studied with **1e**. Whether such curvature also exists for **1b–d** has not been determined, since there are practical limits (at least at 28.5 °C) to the pK range accessible to study. It is interesting, but probably coincidental, that the Brønsted slopes for **1b**, **1c**, and **1d** intersect at ca. pK = 1 (Figure 2). Further, there is a steady decrease in the value of α with decreasing degree of alkylation in the homophthalic acid. This gradation may be related to a decreasing basicity in the benzoic acid carbonyl group, or to a decreasing stabilization of an acylium ion intermediate, or both.

Figure 2 shows that the spread in specific rate constants (**1a–f**) increases with increasing catalyst acidity. We have chosen, therefore, to examine the rate enhancements factors (Table VI) under the most favorable circumstances. There is insufficient data to establish a Hammett ρ value for the electronic effects of the aromatic methyl groups; a rough estimate (from earlier studies) suggest that the k_1 value for **1f** should be reduced by a factor of ca. 2 to adjust for electronic effects. In any case, it is evident that a significant rate-enhancement effect already exists for **1e**, and that the additional methyl group at C-3 (in **1f**) further increases k_1 by a factor less than 10. In order to evaluate the significance of anhydride ring size, we have compared the literature data for 3,6-dimethylphthalic acid[8] with that for **1d**. The value of K_{eq} for the phthalic acid, 0.20 in water at 60 °C, is fairly close to that for **1d**, 0.09 in acetonitrile at 28.5 °C. The specific rate constant for cyclization of the phthalic acid in 0.1 M hydrochloric acid at 28.5 °C is estimated to be 0.10 M^{-1} min^{-1} (extrapolated from data at 60 °C); the value of k_1 for **1d** in acetonitrile (with perchloric acid catalysis) is 0.12 M^{-1} min^{-1}. Thus, we may tentatively conclude that the increased possibilities for conformational flexibility (and wider population distribution) inherent in the homophthalic acids are essentially balanced by the reduction in strain associated with formation of the larger anhydride ring.

The very small variations in k_{obsd} for hydrolysis of the anhydrides in aqueous acid suggest that the free-energy contents of the cyclic species may be nearly equivalent. Roughly quantitative free energy diagrams (Figure 9) can be constructed on the basis of equilibrium and rate data (both for cyclization and hydrolysis), based on the assumption that E_a (for perchloric acid catalysis) is the same for **1a** and **1f**. The diagrams show that the free energy content of

(34) (a) Bloomfield, J. J.; Lees, S. L. *J. Org. Chem.* **1967**, *32*, 3919. (b) Bailey, D. M.; Johnson, R. E. *Ibid.* **1970**, *35*, 3574.

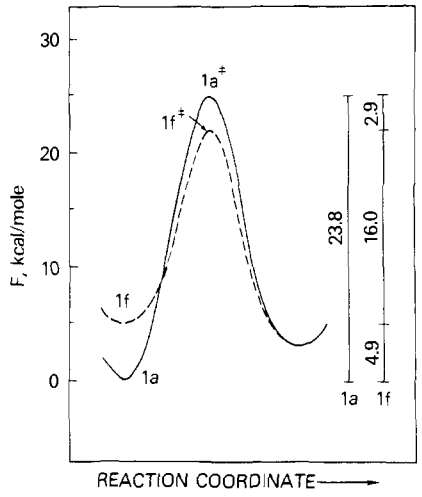

Figure 9. Free energy diagrams showing relationships between ΔF and $\Delta F^{\ddagger}$ for **1a**/**2a** and **1f**/**2f**. The free energy contents of **2a** and **2f** are assumed equivalent.

1f is 4.9 kcal/mol greater than that of **1a**, that for **1f**‡ is 2.9 kcal/mol less than that for **1a**‡, and $\Delta F^{\ddagger}$ for cyclization of **1f** (with perchloric acid catalysis) is 7.8 kcal/mol less than that for **1a**. Thus, of the total reduction in $\Delta F^{\ddagger}$ for **1f**, ca. 63% is due to an increase in the free energy content of the conformationally restricted homophthalic acid, and 37% is due to a reduction in the free energy content of the transition state. In a similar analysis for **1e** vs. **1a**, a net reduction of 6.6 kcal/mol in $\Delta F^{\ddagger}$ can be divided into a 3.4-kcal change in the ground state and 3.2 kcal in the transition state.

If the entire series of homophthalic acids does follow path A with strong acid catalysis, the pattern of rate enhancement (Table VI, column 5) may reflect contributions from at least three sources: (1) an increasing ground-state population of molecules with cisoid (productive) conformations; (2) an increasing facility to relieve crowding between the carboxyl groups by formation of an acylium ion; (3) an increasing drive to relieve steric crowding between the *gem*-dimethyl group and the proximate C-3 methyl group by ring formation.[8,35] X-ray data indicate that, in the crystal, the aliphatic carboxyl group of homophthalic aciid occupies a position far distant from the aromatic carboxyl group or from its anion.[36] Assuming that nonbonded interactions in the crystal and in solution are comparable, a fully extended (transoid, nonproductive) rotamer (**1a**′) should be thermodynamically preferable to **1a**″ (Figure 10). For **1e**, we consider **1e**′ and **1e**″ as extreme alternatives. The rate enhancement factor, **1e**/**1a** > 10^4, is most reasonably explained by assuming a conformation close to **1e**′ to be heavily preferred. The implication that a gauche equatorial COOH/COOH interaction should be preferred over COOH/CH_3 is supported by axial–equatorial equilibrium data for monosubstituted cyclohexanes.[37] For **1f**, we consider conformations **1f**′ and **1f**″ rather unlikely and believe that the ground state may be distributed between **1f**‴ and **1f**⁗.[38] A preference for cisoid rotamers in the solid state has already been shown by X-ray analysis for reasonably analogous phenolic systems.[39] The NMR δ values for the *gem*-dimethyl groups in **1e** or **1f**, or that for the 3-methyl group in **1f**, are not significantly shifted upon addition of base; apparently, the CH_3/COOH gauche interaction is less acceptable than even two proximate carboxylate ions.

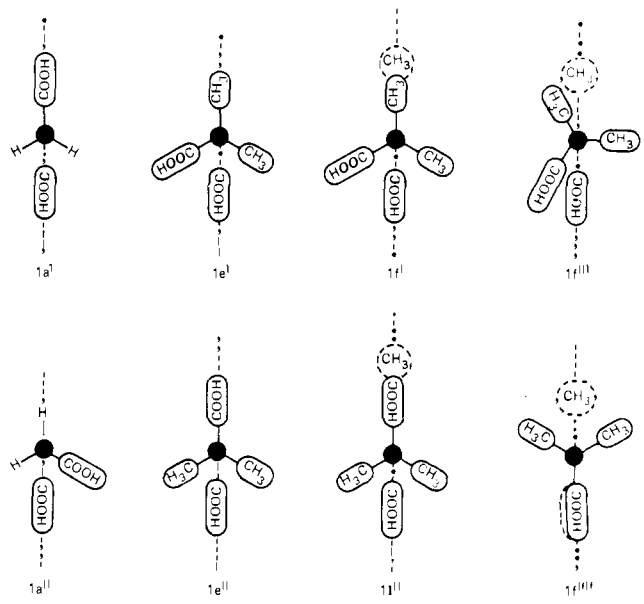

Figure 10. Edge views of productive and nonproductive rotamers of **1a**, **1e**, and **1f**.

The evidence for acylium ion formation has already been presented and discussed; although this pathway is normally observed as the result of crowding in ortho-substituted benzoic acids, we now argue that a more distant, but conformationally constrained, substituent (e.g., another carboxyl group as in **1e**′) can achieve the same effect. The modest increase in values of K_{eq} and of k_1 for **1f** vs. **1e** may, indeed, result from some relief of steric crowding by cyclization (factor 3). The principal rate enhancement effect, however, occurs between **1a** and **1e** (6.6×10^4), and it is rather difficult to visualize the C-3 hydrogen atom (in **1e**) as a source of steric crowding.

In the case of weak acid catalysis (path B), formation or breakdown of a tetrahedral intermediate might be considered an alternative to acylium ion formation as a means to relieve crowding between gauche carboxyl groups; however, the absence of steric effects in ring opening, as well as the selective methanolysis and hydride reduction of the aliphatic carbonyl group in the anhydride, mitigate against consideration of this as a major factor in rate enhancement for cyclization.

Although substrate pK values were not involved in rate or equilibrium calculations, we felt such data might reflect conformational differences in the series. For **1a**, $pK_1 = 3.72$ and $pK_2 = 4.56$. *o*-Alkylbenzoic acids have anomalously low pK values because of steric inhibition of resonance (Table IV, reference in footnote *a*), and this pK_1 values compares favorably with that of 2-ethylbenzoic acid (3.77). The pK_2 value is 0.25 unit higher than that of phenylacetic acid (4.31), owing to the electronic and electrostatic effects of the aromatic carboxylate ion. For **1f**, $pK_1 = 3.59$ and $pK_2 = 5.05$; any conformational constraints imposed on **1f** do not appear to perturb pK_1 to any extent. For pK_2, we estimate a value of 4.50; the observed value is 0.55 unit higher than that estimated, and the additional perturbation (relative to **1a**) is assumed to result from an enforced proximity to the aromatic carboxylate ion.

The data of Figure 2 show that the large spread in values of k_1 observed for perchloric acid catalysis (path A) of homophthalic acid cyclization is greatly reduced with decreasing catalyst efficiency and, if continued extrapolation of the Brønsted slopes were valid, the spread could become trivial. In fact, the nonparallelism of these slopes leads to the remarkable possibility that, for very weak catalyst acids, the order of rate enhancement could even be reversed! This unlikely consequence suggests that the Brønsted plots for all members of the series would show curvature in some intermediate catalysis region and become roughly parallel as path B assumes the major role in cyclization. Unfortunately, the requisite kinetic data ($K_T k_4$) cannot be acquired under convenient

(35) Danforth, C.; Nicholson, A. W.; James, J. C.; Loudon, G. M. *J. Am. Chem. Soc.* **1976**, *98*, 4275.
(36) (a) Gupta, M. P.; Sahu, M. *Acta Crystallogr., Sect. B* **1971**, *27*, 2469; **1972**, *28*, 2887. (b) Gupta, M. P.; Dubey, D. S. *Ibid.* **1972**, *28*, 2677.
(37) Ferguson, L. N. "Organic Molecular Structure"; Willard Grant Press: Boston, Mass., 1975; p 471. Eliel, E. L.; Allinger, N. L.; Angyal, S. J.; Morrison, G. A. "Conformational Analysis"; Interscience: New York, 1966; p 44.
(38) Throughout the series, the steric effects of a solvated acylium ion are assumed to parallel those of the benzoic carboxyl group.
(39) Karle, J. M.; Karle, I. L. *J. Am. Chem. Soc.* **1972**, *94*, 9182.

experimental conditions, if at all. Nevertheless, the trend in Brønsted slope within a given series may provide useful information on uniformity or change in mechanism as rotation barriers are introduced progressively.[6b] There are, undoubtedly, earlier studies in which significant conformation effects on mechanism have escaped detection because the reaction conditions chosen for study were not the most revealing.[2] Thus, the possibilities of concurrent and competitive reaction pathways, in addition to any number of other complicating factors, make the quantitative interpretation of propinquity and other intramolecular phenomena both painstaking and hazardous.

Experimental Secton[40]

6-Methylhomophthalic Acid (1b) and Its Anhydride (2b). Diethyl malonate was alkylated with *o*-methylbenzyl bromide (Aldrich).[41,42] The product was hydrolyzed and decarboxylated to β-(*o*-tolyl)propionic acid,[42] and the latter compound was cyclized with polyphosphoric acid to 4-methyl-1-indanone,[42-44] IR ($CHCl_3$) 1710 cm^{-1}. The indanone was oximinated with butyl nitrite,[43,44] and the α-oximino ketone was hydrolyzed in the presence of formaldehyde to 4-methyl-1,2-indandione.[44] The diketone, without isolation, was oxidized with acidified hydrogen peroxide[44] to 6-methylhomophthalic acid (**1b**), mp 194–196 °C (lit.[44] mp 195–196 °C). The diacid was cyclized with acetyl chloride to the anhydride (**2b**), mp 149–150 °C (benzene) (lit.[44] mp 150 °C), IR ($CHCl_3$) 1755 and 1800 cm^{-1}.

3-Methylhomophthalic Acid (1c) and Its Anhydride (2c). β-(*m*-Tolyl)propionic acid[45] was prepared from *m*-methylbenzyl bromide by the procedure cited above for the ortho isomer.[41,42] The acid was cyclized with polyphosphoric acid to a mixture of 5-methyl- and 7-methyl-1-indanone,[45,46] the latter ketone being recovered by silica gel chromatography, mp 51.5–52.5 °C (lit.[45] mp 52.5–53.5 °C). The ketone was subjected to Claisen condensation with diethyl oxalate in benzene,[47] sodium hydride being used as the condensing agent. The yellow sodium enolate (from 0.1 mol of 7-methyl-1-indanone) was collected by filtration, washed with ether, and dissolved in a mixture of 50 mL of water and 200 mL of methanol. To the light brown solution was added 4.5 g (0.11 mol) of sodium hydroxide, followed by rapid addition of a solution of 75 mL of hydrogen peroxide (30%) in 50 mL of methanol. The mixture was stirred until the color was discharged and then heated on steam for 0.5 h. Methanol was removed under reduced pressure, and the aqueous solution was acidified with concentrated hydrochloric acid; it was then extracted with ethyl acetate (3 × 150 mL) and chloroform (100 mL). The combined extracts were dried ($MgSO_4$) and concentrated to 100 mL. The solution was decolorized with charcoal (hot); the filtrate was further concentrated to 25 mL, then diluted with 75 mL of petroleum ether (bp 30–60 °C), and refrigerated overnight. Filtration provided 1.34 g (67% based on the indanone) of a colorless solid, mp 140–141 °C. Recrystallization from ethyl acetate–hexane gave **1c**, mp 141–142 °C. Anal. ($C_{10}H_{10}O_4$) C, H.

A solution of **1c** in acetyl chloride was heated at reflux for 1 h, the solvent was removed in vacuo, and the residue was crystallized from ethyl acetate–hexane to give **2c**, mp 94–95 °C, IR ($CHCl_3$) 1755 and 1800 cm^{-1}. Anal. ($C_{10}H_8O_3$) C, H.

3,6-Dimethylhomophthalic Acid (1d) and Its Anhydride (2d). The Friedel–Crafts reaction between *p*-xylene and β-chloropropionyl chloride was used to prepare 4,7-dimethyl-1-indanone[48] in 75% yield, mp 75–76 °C (lit.[48] mp 76–77 °C). The ketone was oximinated with ethyl or butyl nitrite to the α-oximino ketone[43] in 85% yield, mp 205–207 °C. To a suspension of 2.0 g (0.01 mol) of the oximino ketone in 20 mL of glacial acetic acid were added 10 mL of aqueous formaldehyde (35–40%) and 5 mL of concentrated hydrochloric acid. The compound dissolved within 5 min; the resulting solution was stirred for 3 h (25 °C) and was diluted with ice–water. The yellow, crystalline precipitate was collected by filtration and was recrystallized from ethyl acetate–hexane to give 1.47 g (80%) of 4,7-dimethyl-1,2-indandione, mp 171–175 °C (lit.[49] mp 175–175 °C), IR ($CHCl_3$) 1720 and 1770 cm^{-1}.

To a stirred solution of the indandione in 30 mL of glacial acetic acid was added 0.2 mL of concentrated sulfuric acid, following by 1.5 mL of 30% hydrogen peroxide added dropwise over 1–2 min at 25 °C. The yellow color of the solution disappeared within 5 min and the reaction mixture was stirred 4.5 h at ambient temperature. The solution was diluted with 100 mL of water and, after adjustment to pH 1, was stirred overnight. The mixture was extracted with ether (3 × 125 mL); the combined extracts were dried ($MgSO_4$) and concentrated to a small volume containing residual acetic acid. The solvent was evaporated in a stream of nitrogen, leaving a colorless, crystalline solid which was recrystallized from ethyl acetate–hexane to give 0.88 g (82%) of **1d**, mp 164–165 °C. Anal. ($C_{11}H_{12}O_4$) C, H.

The acid was cyclized with acetyl chloride (as for **1c**) and the product was recrystallized from chloroform–hexane to give **2d**, mp 117–118.5 °C, IR ($CHCl_3$) 1755 and 1790 cm^{-1}. Anal. ($C_{11}H_{10}O_3$) C, H.

3,3-Dimethyl-1-indanone.[50a] A solution of 10.0 g (0.10 mol) of β,β-dimethylacrylic acid in 25 mL of dry benzene was stirred in an ice–salt bath (ca. 5 °C) while 16.0 g (0.12 mol) of anhydrous aluminum chloride was added in small portions over 1 h. The reaction mixture was stirred an additional 2 h at 5 °C and refrigerated for 12 h. Workup of an aliquot of the solution at this point provided β-phenylisovaleric acid, mp 55–60 °C.[50b] The main solution was concentrated at 40 °C to a yellow-brown oil, which was cooled in an ice–salt bath and diluted with 200 mL of cold, concentrated sulfuric acid over 10 min. The reaction mixture was stirred at 5 °C for 25 min and at ambient temperature for 48 h. The solution was poured slowly onto 1 kg of crushed ice, and the mixture was extracted with ether (3 × 150 mL); the combined ether extracts were washed with 5% sodium bicarbonate and saturated brine and dried ($MgSO_4$). Removal of the solvent gave 10 g of a yellow oil; fractional distillation gave 6.5 g (overall yield 41%) of 3,3-dimethyl-1-indanone, bp 66–68 °C (0.3 mm).[51] Identity of the cyclic ketone was verified by spectral data: IR ($CHCl_3$) 1710 cm^{-1}; NMR ($CDCl_3$) δ 1.42 (s, 6, CH_3's), 2.57 (s, 2, CH_2), 7.5 (m, 4, aryl H's).

α,α-Dimethylhomophthalic Acid (1e) and Its Anhydride (2e). To 50 mL of dry benzene was added, at 0–5 °C under nitrogen, 0.63 g of sodium hydride (0.015 mol, 57% dispersion in mineral oil). To the stirred mixture was added dropwise over 1 h a solution of 2.0 g (0.012 mol) of 3,3-dimethyl-1-indanone in 50 mL of benzene. A solution of 2.0 g (0.014 mol) of diethyl oxalate in 30 mL of benzene was then added over 15 min. The reaction mixture was allowed to warm to ambient temperature and was stirred 15 h. The yellow-brown solution was concentrated in vacuo and the sodium enolate was precipitated with petroleum ether. The yellow product was collected by filtration and was washed with petroleum ether. The enolate salt was dissolved directly in 150 mL of hot methanol; to the brown solution was added 5 g (0.125 mol) of sodium hydroxide and 10 mL of water. To the rapidly stirred solution was added, over 5 min, 100 mL of 30% hydrogen peroxide. The solution, which had decolorized rapidly, was stored at ambient temperature for 15 min and then heated at reflux for 30 min. The solution volume was reduced to 100 mL; crushed ice was added, followed by sufficient concentrated hydrochloric acid to bring the pH to 2–3. The cold solution was extracted immediately with ethyl acetate (3 × 150 mL); the combined extracts were washed with saturated brine and dried ($MgSO_4$) and then concentrated to an oil which crystallized upon addition of petroleum ether. Recrystallization from warm ethyl acetate–petroleum ether (after decolorization with charcoal) afforded 0.78 g (33%) of **1e**, mp 122–123 °C (lit.[52] mp 123 °C). The NMR spectrum ($CDCl_3$) showed methyl signals at 1.72 and 1.77 ppm; within 30 min, these signals coalesced to a single peak at 1.75 ppm, the result of cyclization to the anhydride **2e**, IR (CH_3CN) 1730 cm^{-1}; the mass spectrum showed **1e** and **2e** in the ratio 1:7.

In an alternative route, the 1-indanone was converted to the indandione via the oximino ketone,[53a] and the diketone was oxidized to **1e** with

(40) Microanalyses and mass spectral measurements were performed by the Microanalytical and Instrumentation Section of this laboratory, under the direction of Dr. D. F. Johnson. Melting points and boiling points are uncorrected. In addition to elemental analysis, identity and homogeneity of each compound were checked by NMR and mass spectrometry, and by TLC.

(41) Kaiser, C.; Leonard, C. A.; Heil, G. C.; Lester, B. M.; Tedeschi, D. H.; Zirkle, C. L. *J. Med. Chem.* **1970**, *13*, 820. Elsner, B. B.; Parker, K. J. *J. Chem. Soc.* **1957**, 592.
(42) Dev, S. *J. Indian Chem. Soc.* **1955**, *32*, 403.
(43) Simchen, G.; Krämer, W. *Chem. Ber.* **1969**, *102*, 3656.
(44) Mercer, D.; Robertson, A. *J. Chem. Soc.* **1936**, 288.
(45) House, H. O.; Schellenbaum, M. *J. Org. Chem.* **1963**, *28*, 34.
(46) Granger, R.; Orzalesi, H.; Muratelle, A. *C. Rend. Acad. Sci.* **1961**, *252*, 1971. See also Thorsett, E. D.; Stermitz, F. R. *Syn. Commun.* **1972**, *2*, 375.
(47) Eichenberger, J. *Helv. Chim. Acta* **1948**, *31*, 1663.
(48) Hart, R. T.; Tebbe, R. R. *J. Am. Chem. Soc.* **1950**, *72*, 3286.
(49) Cava, M. P.; Little, R. L.; Napier, D. R. *J. Am. Chem. Soc.* **1958**, *80*, 2257.
(50) (a) This procedure is a modification of that described for higher homologues by Smith, L. I.; Spillane, L. J. *J. Am. Chem. Soc.* **1943**, *65*, 204. See also Ulrich, L.; Hansen, H.-J.; Schmid, H. *Helv. Chim. Acta* **1970**, *53*, 1328. (b) Whitmore, F. C.; Weisgerber, C. A.; Shabica, A. C. *J. Am. Chem. Soc.* **1943**, *65*, 1469.
(51) Pearson, B. D.; Ayer, R. P.; Cromwell, N. H. *J. Org. Chem.* **1962**, *27*, 3038. These authors report bp 101–103 °C (1.5 mm).
(52) Cromwell, N. H.; Campbell, R. D. *J. Org. Chem.* **1957**, *22*, 520. See also Gabriel, S. *Chem. Ber.* **1887**, *20*, 1198.
(53) (a) Koelsch, C. F.; Le Claire, C. D. *J. Org. Chem.* **1941**, *6*, 516. (b) Colonge, J.; Weinstein, G. *Bull. Soc. Chim. Fr.* **1951**, 820.

hydrogen peroxide.[44] The diacid was also prepared, in low yield, by Friedel–Crafts alkylation of toluene with methacrylic acid, and oxidation of the product with alkaline permanganate.[53b]

The anhydride, **2e** formed spontaneously when a chloroform solution of **1e** was stored overnight at 25 °C. The product was recrystallized from hot petroleum ether, mp 79–80 °C (lit.[54] mp 80–81 °C), IR ($CHCl_3$) 1750 and 1790 cm^{-1}.

3,3,4,5,7-Pentamethyl-1,2-indandione. 2′,3,4′,5′-Tetramethylcrotonophenone was prepared in 89% yield (bp 138–141 °C (6 mm)) by Friedel–Crafts acylation of 1,2,4-trimethylbenzene with 3,3-dimethylacryloyl chloride.[55] The unsaturated ketone was cyclized with concentrated sulfuric acid to 3,3,4,5,7-pentamethyl-1-indanone in 91% yield (bp 140–141 °C (5 mm)). This indanone was converted into the α-oximino ketone with butyl nitrite[56] in 67% yield (mp 209–211 °C), and the latter was converted into the indandione in 89% yield, mp 126–127 °C (hexane), IR ($CHCl_3$) 1700 and 1760 cm^{-1}. Anal. ($C_{14}H_{16}O_2$) C, H.

4,4,5,6,8-Pentamethylhomophthalic Anhydride (2f). To a stirred solution of 8.0 g (0.037 mol) of the pentamethylindandione in 150 mL of glacial acetic acid was added 0.5 mL of concentrated sulfuric acid, followed by 11 mL of 30% hydrogen peroxide added dropwise over 10 min.[57] The yellow color was discharged within 2 h, and stirring was continued for a total of 4 h. The volume was reduced to ca. 100 mL, ice was added, and the precipitate was collected by filtration to give 7.2 g (84%) of **2f**, mp 126–127 °C (hexane): IR ($CHCl_3$) 1740 and 1785 cm^{-1}; NMR (CD_3CN) δ 1.80 (s, 6, 4-CH_3's), 2.32 and 2.47 (2s, 6,6- and 8-CH_3's), 2.57 (s, 3, 5-CH_3), 7.19 (s, 1, H-7). Anal. ($C_{14}H_{16}O_3$) C, H.

α,α,3,4,6-Pentamethylhomophthalic Acid (1f). A suspension of **2f** (0.75 g) in 25 mL of 0.5 N sodium hydroxide was heated on steam until solution was complete (ca. 20 min). The solution was cooled and extracted with ether. The aqueous layer was chilled by addition of ice, acidified with 6 N hydrochloric acid, and immediately reextracted with ether (3 × 150 mL). The ether extract was dried ($MgSO_4$) and concentrated to a small volume. Crystallization was effected by slow addition of 75 mL of hexane, and, after chilling, the product was collected and washed with carbon tetrachloride (87% yield). The compound recyclized to **2f** during attempts to determine a melting point: NMR (DMF-d_7) δ 1.60 (s, 6, α,α-CH_3's), 2.15 and 2.25 (2s, 9, 3-, 4-, and 6-CH_3's), 7.04 (s, 1, H-5). Prior to kinetic runs, the solid diacid was washed with carbon tetrachloride to remove any anhydride formed during storage. Anal. ($C_{14}H_{18}O_4$) C, H.

Dimethyl Ester of 1f. The homophthalic acid was esterified with diazomethane in ether. After the solution was dried ($MgSO_4$) and the solvent evaporated, an oil was obtained which crystallized from hexane, mp 175 °C: IR ($CHCl_3$) 1725 cm^{-1}; NMR ($CDCl_3$) δ 1.60 (s, 6, α,α-CH_3's), 2.04 (s, 3, ?-CH_3), 2.22 (s, 6, ?-CH_3's), 3.67 (s, 3, aliphatic OCH_3), 3.87 (s, 3, aromatic OCH_3), 6.97 (s, 1, H-5). Anal. ($C_{16}H_{22}O_4$) C, H.

Monomethyl Ester of 1f. A solution of 0.20 g (0.86 mmol) of **2f** in 15 mL of methanol (to which has been added 25 mg of sodium) was heated at reflux for 1 h. The solution was concentrated to 1–2 mL and 10 mL of ether was added. The solution was chilled in ice until crystallization began; an additional 50 mL of ether was added and the solid was collected. The sodium salt was dissolved in warm water; the solution was acidified with 6 N hydrochloric acid and extracted with ether. The extract was dried ($MgSO_4$) and concentrated to an oil which solidified under cold hexane. Recrystallization from ethyl acetate–hexane gave 0.072 g (32%) of the monomethyl ester, mp 112–113 °C: IR ($CHCl_3$) 1725–1730 cm^{-1}; NMR ($CDCl_3$) δ 1.74 (s, 6, α,α-CH_3's), 2.07 and 2.26 (2s, 6, 4- and 6-CH_3's), 2.36 (s, 3, 3-CH_3), 3.72 (s, 3, OCH_3), 7.02 (s, 1, H-5). Anal. ($C_{15}H_{20}O_4$) C, H.

The methyl proton signals of simple aliphatic methyl esters are found at δ 3.6–3.7 while those of methyl benzoates fall in the range 3.8–3.9. This distinction is clear in the dimethyl ester of **1f** (δ 3.67 and 3.87) and in that of **1a** (3.71 and 3.87). The value for the monomethyl ester of **1f** shows clearly that it is the aliphatic ester. The p*K* value of the monomethyl ester, 3.74, is also consistent with that of a free benzoic acid. The crystallization mother liquors gave no evidence for the presence of the isomeric methyl ester. On prolonged storage, solid samples of the monomethyl ester revert slowly to the anhydride. In the presence of 0.02 M $HClO_4$ in acetonitrile, the same conversion occurs with $t_{1/2}$ = 4–5 min; in this medium, $t_{1/2}$ for cyclization of **1f** is estimated at 2 s.

Borohydride Reduction of 2f. Sodium borohydride (0.24 g, 6.4 mmol) was added to 20 mL of dry tetrahydrofuran and the mixture was stirred at ambient temperature.[34b] After 20 min, a solution of 0.30 g of **2f** in 15 mL of tetrahydrofuran was added dropwise over 20 min. The reaction mixture was stirred for 24 h and most of the solvent was evaporated; the residual material was diluted with water and the solution was acidified to pH 1–2 with dilute hydrochloric acid. The solution was extracted with ether (3 × 75 mL), the combined extracts were dried ($MgSO_4$) and concentrated to a partially solid residue. This material was extracted with hexane and the extract was concentrated to a sweet-smelling oil. Preparative TLC (silica gel, ether–hexane 3:7) provided 50 mg of an oil: *m/e* 219 (M + 1); IR ($CHCl_3$) 1710 cm^{-1}; NMR (CCl_4) δ 1.48 (s, 6, 4,4-CH_3's), 2.26, 2.30 (2s, 6, 6- and 8-CH_3's), 2.52 (s, 3, 5-CH_3), 3.88 (s, 2, CH_2), 6.95 (s, 1, H-7). An upfield shift of 24 Hz for the *gem*-dimethyl group (relative to **2f**) indicates that reduction had occurred at the C-3 carbonyl .

Homoconjugate Salts. The acid salts were prepared by addition of an excess of the carboxylic acid to an ethanolic solution of tetra-*n*-butylammonium ethoxide, as described for the acetate complex.[58] Salts were also prepared from the following acids (all gave acceptable C, H, and N analyses): CF_3COOH, mp 66–68 °C (chloroform–hexane); CH_3OCH_2COOH, bp > 150 °C (analytical sample contained 1 mol of water); $ClCH_2COOH$, bp >100 °C. Neutralization of tetra-*n*-butylammonium hydroxide with 1 equiv of cyanoacetic acid gave the simple salt, bp >100 °C (analytical sample contained 1.5 mol of water). Ths material was also used for kinetic studies; departure from the HA_2^- series did not appear to cause deviations in the kinetic results or in the Brønsted correlation (Figure 7).

Deuterated Acids. Samples of trifluoroacetic and acetic anhydride were hydrolyzed with a slight excess of deuterium oxide (99.7%) and the deuterated acids were stored over freshly activated molecular sieve.

p*K* Determinations. Titrations were performed at 25 °C in water containing 4–5% dioxane. The overlapping p*K*'s were resolved by Martin's procedure:[59] benzoic acid, 4.22; phenylacetic acid, 4.31; homophthalic acid, 3.72 and 4.56; **1f**, 3.59 and 5.05; **1f** monomethyl ester, 3.74.

Kinetic and Equilibrium Measurements. Solvent acetonitrile was purified by three distillations from phosphorus pentoxide and stored over molecular sieve (under nitrogen). The water content of catalyst acids was determined by titration of weighed samples with standard base. The apparatus and kinetic methods have been described previously.[3] The change in absorption was followed at 240–245 and 290–300 nm until constant values were obtained. All rate and equilibrium measurements were performed at 28.5 ± 0.1 °C.

Acknowledgment. We are grateful to Professor W. P. Jencks for his valuable comments and suggestions.

Registry No. 1a, 89-51-0; **1b**, 84944-40-1; **1c**, 84944-41-2; **1d**, 84944-42-3; **1e**, 40484-15-9; **1f**, 84944-43-4; **1f** dimethyl ester, 84944-50-3; **1f** monomethyl ester, 84944-51-4; **2a**, 703-59-3; **2b**, 84944-46-7; **2c**, 84944-47-8; **2d**, 84944-44-5; **2e**, 31952-55-3; **2f**, 84944-45-6; **2f**-ol, 84944-52-5; $HClO_4$, 7601-90-3; CH_3SO_3H, 75-75-2; CF_3COOH, 76-05-1; HCF_2COOH, 381-73-7; HC≡CCOOH, 471-25-0; $NCCH_2COOH$, 372-09-8; $ClCH_2COOH$, 79-11-8; CH_3OCH_2COOH, 625-45-6; CH_3COOH, 64-19-7; $CF_3CO_2^-Bu_4N$, 39481-22-6; $ClCH_2CO_2^-Bu_4N$, 18819-88-0; $CH_3OCH_2CO_2^-Bu_4N$, 60154-70-3; deuterium, 7782-39-0; 7-methyl-1-indanone, 39627-61-7; diethyl oxalate, 95-92-1; 4,7-dimethyl-2-(hydroxyimino)-1-indanone, 24623-36-7; 4,7-dimethyl-1,2-indandione, 73356-55-5; β,β-dimethylacrylic acid, 541-47-9; β-phenylisovaleric acid, 1010-48-6; 3,3-dimethyl-1-indanone, 26465-81-6; 3,3,4,5,7-pentamethyl-1,2-indandione, 84944-48-9; 3,3,4,5,7-pentamethyl-1-indanone, 10425-83-9; 3,3,4,5,7-pentamethyl-2-(hydroxyimino)-1-indanone, 84944-49-0.

(54) Kloetzel, M. C. *J. Am. Chem. Soc.* **1940**, *62*, 3405.
(55) Bansal, R. C.; Mattox, J. R.; Eisenbraum, E. J. *J. Org. Chem.* **1966**, *31*, 2716. See also Smith, L. I.; Prichard, W. W. *J. Am. Chem. Soc.* **1940**, *62*, 771.
(56) Eistert, B.; Witzmann, H. K. *Justus Liebigs Ann. Chem.* **1971**, *744*, 105.
(57) Prinzbach, H.; Vogel, P.; Auge, W. *Chimia* **1967**, *21*, 468.
(58) Crampton, M. R.; Grunwald, E. *J. Am. Chem. Soc.* **1971**, *93*, 2990.
(59) Martin, R. B. *J. Phys. Chem.* **1971**, *75*, 2657. See also Albert, A.; Serjeant, E. P. "Ionization Constants of Acids and Bases"; Wiley: New York, 1962; p 51.